

Fig. 3. Comparison of response of RNN-PNN filter and PCLPF.

and RNN-PNN system for one of the flux channels. These outputs were equally scaled before plotting for clarity. The responses are identical in steady state, but there is a difference in transient response. The PCLPF presents a sharp discontinuity at the transient response, whereas the RNN-PNN response is gradual. The objective of the filter is to achieve an operation approaching that of an ideal integrator. Therefore, it can be seen, from the transient response shown in Fig. 3, that the smoother response of the RNN-PNN will be more precise, doing the job, than the PCLPF. The estimated time to run the RNN-PNN filter, using DSP type TMS320C30, is around 13.5  $\mu$ s.

### VIII. CONCLUSION

PCLPF-based stator flux vector synthesis was successfully replaced by an RNN where the network weights as a function of frequency were updated by another feedforward polynomial-type neural network. The RNN structure was derived on the basis of a two-stage filter, and was trained by a Kalman filter. The whole RNN-PNN flux vector estimator was evaluated extensively in the frequency range of 0.01–200 Hz and showed improved performance. The proposed flux estimator is simpler and easier to implement in the DSP. The estimator can also be used for rotor-flux-oriented vector control, as well as a direct-torque-control-based control system.

### REFERENCES

- [1] B. K. Bose and N. R. Patel, "A programmable cascaded low-pass filter-based flux synthesis for a stator flux-oriented vector-controlled induction motor drive," *IEEE Trans. Ind. Electron.*, vol. 44, pp. 140–143, Feb. 1997.
- [2] —, "A sensorless stator flux oriented vector controlled induction motor drive with neuro-fuzzy based performance enhancement," in *Conf. Rec. IEEE-IAS Annu. Meeting*, 1997, pp. 393–400.
- [3] K. S. Narendra and K. Parthasarathy, "Identification and control of dynamic systems using neural networks," *IEEE Trans. Neural Networks*, vol. 1, pp. 4–27, Jan. 1990.
- [4] G. V. Puskorius and L. A. Feldkamp, "Neurocontrol of nonlinear dynamic systems with Kalman filter trained recurrent networks," *IEEE Trans. Neural Networks*, vol. 5, pp. 279–297, Mar. 1994.
- [5] A. P. A. Silva, P. C. Nascimento, G. L. Torres, and L. E. Borges da Silva, "Alternative approach for adaptive real-time control using a nonparametric neural network," in *Conf. Rec. IEEE-IAS Annu. Meeting*, 1995, pp. 1788–1794.

## A Startup Control Algorithm for the Split-Link Converter for a Switched Reluctance Motor Drive

Y. Liu and P. Pillay

**Abstract**—This letter analyzes and presents the motor startup problem when a split-link converter is used for switched reluctance motor drives. A new control algorithm to solve this problem is presented in this paper, as well as the calculation of the split-link capacitance required during normal operation.

**Index Terms**—DC-link capacitance, multiphase operation.

### I. INTRODUCTION

The switched reluctance motor (SRM) has advantages of mechanical and thermal robustness, ease of manufacture, and high-speed capability over squirrel-cage induction motors [1]. It is, therefore, attracting considerable research interest, as well as the attention of manufacturers. Four types of converters are widely used in SRM drives: the classic converter with  $2n$  active switches, the  $n + 1$  switch converter, the C-dump converter, and the split-link converter. The split-link converter has the advantage of the lowest component number, when compared to the other types [2] and is, therefore, available commercially. While there is very little existing literature on this converter, some drawbacks are mentioned in [2]. These include the reduced ability for soft chopping and the difficulties associated with maintaining voltage balance between phases. It can be only used in SRM drives with an even phase number. For industrial applications, there are additional considerations. Since two capacitors divide the dc-link voltage in two and each capacitor provides the phase voltage, the conduction of a phase causes ripple in the capacitor voltage. At startup and low-speed operation, the problem is more severe. It is quite possible that the motor does not start. This letter analyzes this problem and presents a new algorithm to solve this problem, as well as the calculation of the capacitance required for the split-link converter to operate satisfactorily over its speed range.

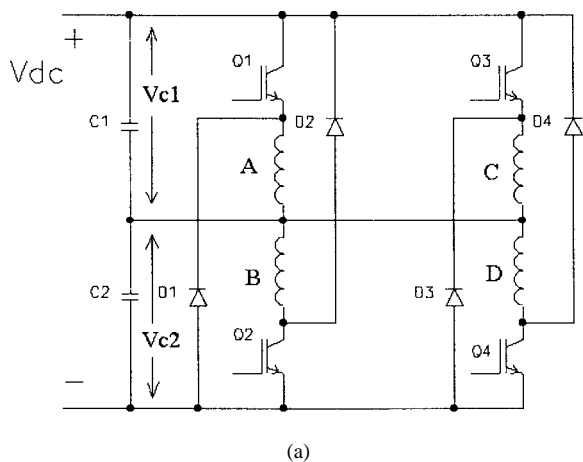
### II. VOLTAGE RIPPLE ANALYSIS AND THE STARTUP ALGORITHM

The converter circuit for a four-phase drive is shown in Fig. 1(a). The two capacitors act like two dc power supplies for the upper two phases and the lower two phases. When  $Q1$  is turned on, current flows through  $Q1$  and phase A.  $C1$  is, therefore, being discharged and  $C2$  is being charged, as shown in Fig. 1(b). When  $Q1$  is turned off, the current in phase A goes through  $D1$  and  $C2$ , hence,  $C2$  is charged again and  $V_{c2}$  increases further. A similar procedure occurs when phases B, C, and D are excited. During normal operation, the conducting phase shifts between the upper leg and the lower leg, and the capacitors are charged and discharged in turn, so that the capacitor voltages remain relatively stable. However, at low speed, the frequency of shifting between the upper leg and the lower leg is low, so that the voltage of the capacitor can drop significantly. Fig. 2(a) shows the currents of phases A and C and the voltage of  $C2$  at an operating speed of 79 r/min with  $15^\circ$  (mechanical degrees)

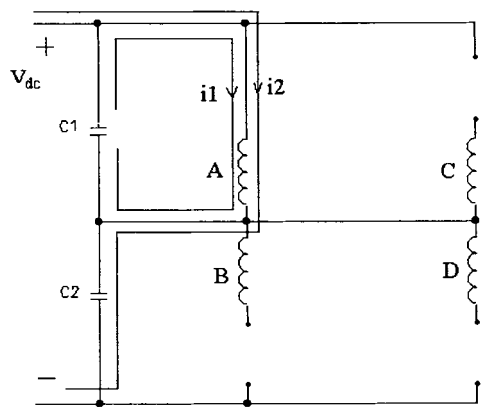
Manuscript received March 30, 1998; revised February 4, 1999. Abstract published on the Internet March 1, 1999.

The authors are with the Department of Electrical and Computer Engineering, Clarkson University, Potsdam, NY 13699-5720 USA (e-mail: pillay@sun.soe.clarkson.edu).

Publisher Item Identifier S 0278-0046(99)04151-9.



(a)



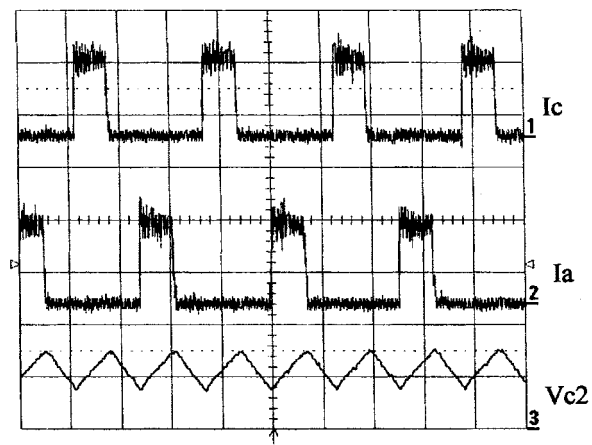
(b)

Fig. 1. (a) Split-link converter for the SRM drive. (b) Phase A currents during turn-on.

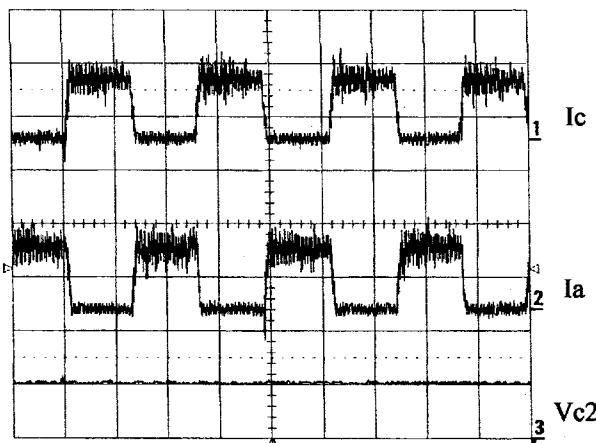
conduction angle for a 4-kW 8/6 SRM which is rated at 300 V, 8 A, and 1500 r/min. There is almost a 75% ripple voltage in  $V_{c2}$ . At startup, it can be even worse. When the load is heavy, the voltage across one capacitor can drop to zero before the rotor can move to the next phase, and the motor will not start at all. In addition, the voltage across the complementary capacitor can reach the full dc-link voltage, at which point the rated values of the capacitors and transistors can be exceeded.

To avoid this problem, a new control algorithm for the startup and low-speed operation of a split-link converter is presented here. The new scheme allows two phases to conduct at the same time during startup, i.e., there is always an upper leg and a lower leg conducting. The conducting sequences are  $AB, BC, CD, DA, AB, \dots$ , or the reverse for opposite direction operation, as shown in Fig. 3. In each mode, there is a path for the current flowing from the positive terminal of the dc supply through the two phases to the negative terminal. Each phase conducts for  $30^\circ$ . This method thus uses the entire positive-torque-producing region of  $30^\circ$  for the 8/6 SRM. The currents and the voltage across one capacitor are shown in Fig. 2(b) with the motor running at 79 r/min. The voltage ripple was reduced significantly. With this method, the motor can start at any position, even under heavy load.

For the  $30^\circ$  conduction region, the torque per ampere is low around the aligned and unaligned positions, so the efficiency during startup is not optimal. This is a tradeoff disadvantage for the split-link converter. The torque ripple of this method at startup is around 37% (peak-to-peak/average). Zero torque ripple can be achieved with the



(a)



(b)

Fig. 2. (a) Voltage ripple at low-speed operation. (b) New control algorithm at low speed. Trace 1: phase C current, 2 A/div; trace 2: phase A current, 2 A/div; and trace 3:  $V_{c2}$ , 50 V/div.

	0	30	60	90
	A	C	A	C
	D	B	D	B
	15	45	75	105

Fig. 3. Conducting angles (mechanical degrees).

classic SRM converter, theoretically, by using proper control. However, this torque ripple mitigation algorithm cannot be implemented on the split-link converter at startup.

### III. CAPACITOR CALCULATION FOR NORMAL SPEED OPERATION

After the speed increases to a suitable value, other control schemes can be applied, such as conducting angle control and current shaping, for maximum efficiency or smooth torque. At higher speeds, the conducting angle need not necessarily be  $30^\circ$ , with the result that voltage ripple will occur in  $V_{c1}$  and  $V_{c2}$ . In most cases, the ripple is required to be within a certain limit for desired performance. The ripple is a complicated function of the capacitance, dc voltage, turn-on and turn-off angles, load torque, etc.

Suppose phase *A* is turned on and  $V_{c1}$  drops from  $U_1$  to  $U_2$ . The currents are shown in Fig. 1(b). Ignoring the losses in the converter and the motor, the energy received by the motor is

$$\begin{aligned} w_c &= \int_{t_1}^{t_2} (i_1 + i_2)v_{C1} dt \\ &= \int_{t_1}^{t_2} \left( -c_1 \frac{dv_{C1}}{dt} + c_2 \frac{dv_{C2}}{dt} \right) v_{C1} dt \\ &= - \int_{U_1}^{U_2} (c_1 + c_2)v_{C1} dv_{C1} \\ &= (c_1 + c_2)(U_1^2 - U_2^2)/2 \\ &= C(U_1^2 - U_2^2). \end{aligned} \quad (1)$$

Note that  $dv_{C2} = d(V_{DC} - v_{C1}) = -dv_{C1}$ , and  $c_1 = c_2 = C$ .

Part of the energy received by the motor is converted into mechanical work  $w_m$  and the rest is stored in the electromagnetic field  $w_j$ . So,

$$w_c = w_m + w_j = T_l \theta + w_j = C(U_1^2 - U_2^2) \quad (2)$$

where  $\theta$  is the stroke angle, and  $T_l$  is the load torque.

When  $QI$  is turned off, current flows through  $DI$ , phase *A* and  $C2$ . So  $V_{c2}$  increases.  $V_{dc}$  is produced from a bridge rectifier and current cannot flow back to the rectifier. So  $V_{c1}$  does not change. Based on the above analysis, the capacitance can be found for a required voltage ripple. For the worst case consideration,  $w_j$  should be taken as the maximum energy the motor can store within the motor ratings. As an approximation,  $w_j$  can be taken as  $2 w_m$ . For the 8/6 4-kW motor at rated torque, if the phase voltage ripple of  $300 \pm 15$  V is required, then capacitors larger than  $710 \mu\text{F}$  are needed in the circuit. In our converter,  $1300\text{-}\mu\text{F}$  capacitors are used. These equations are not valid during startup and low-speed operation, since the losses are much larger.

At the rated speed, with the appropriate value capacitors as calculated above, a control algorithm can be used to improve efficiency and/or reduce torque ripple without concern of voltage ripple. At startup,  $30^\circ$  conduction must be used even though the efficiency is not high. At speeds between these two, the conduction angle can be reduced from  $30^\circ$  for higher efficiency. But some precautions should be taken. A simplified analysis is presented here. For  $30^\circ$  conduction, there is no time during which only one phase is conducting; for  $15^\circ$  conduction, only one phase is conducting.  $15^\circ$  is the minimum conduction angle for normal operation since the stroke angle for an 8/6 SRM is  $15^\circ$ . For a conduction angle  $\alpha$  between  $30^\circ$  and  $15^\circ$ , the region with only one phase conducting is  $30^\circ - \alpha$ , and the corresponding time  $t$  is  $(30 - \alpha)/\omega$ , where  $\omega$  is the speed in mechanical degrees per second. The voltage drop  $\Delta U$  during time  $t$  is

$$\Delta U = \frac{It}{2C} = \frac{I(30 - \alpha)}{2C\omega} \quad (3)$$

where  $I$  is the phase current. For the worst case of  $15^\circ$  conduction angle, for the rated torque and the capacitor value in the converter, for  $300 \pm 15$  V voltage ripple,  $t$  is calculated as 4.9 ms, and the corresponding speed is 510 r/min. So, for a speed greater than 510 r/min, the conduction angle can be controlled freely. After startup, but below 510 r/min, the conduction angle can be reduced from  $30^\circ$ , but it must satisfy the above equation. The calculation for any other SRM will utilize the same equation above, using knowledge of the motor peak current.

#### IV. CONCLUSION

Due to the operational characteristics of the split-link converter for the SRM drive, the voltage ripple in the capacitors can cause a problem at startup or low-speed operation. This letter has presented a control algorithm to solve this problem, and the experimental results have demonstrated its effectiveness. For normal speed operation, the calculation of the capacitance of the converter to meet the voltage ripple requirements was derived. At intermediate speeds, the proper conduction angle requirement has been presented.

#### REFERENCES

- [1] P. J. Lawrenson, J. M. Stephenson, P. T. Blenkinsop, J. Corda, and N. N. Fulton, "Variable-speed switched reluctance motors," *Proc. Inst. Elect. Eng.*, vol. 127, pt. B, no. 4, pp. 253–265, 1980.
- [2] T. J. E. Miller, *Switched Reluctance Motors and Their Control*. Oxford, U.K.: Oxford Univ. Press, 1993.

### A Decomposed Control Scheme for Vision-Guided Manipulators Curve Tracking

Jiang Ping, Hui-tang Chen, Yue-juan Wang, and Jing Lin

**Abstract**—This letter presents a robot control algorithm for vision-guided curve tracking using orthogonal decomposition control method. It was implemented in a glass-cutting direct-drive robot for the drawing curve input with high speed and smooth tracking performance.

**Index Terms**—Decomposition methods, direct-drive robots, robot vision, tracking systems.

#### I. INTRODUCTION

Curve tracking and reproduction is a typical application of robots with vision systems. It has a broad range of industrial applications in different fields, such as visually guided robot arc welding and drawing curve tracers [1]. This letter presents a new algorithm for vision-guided curve tracking. It is installed on a glass-cutting direct-drive (DD) robot. It is well known that the window glass of a car is made from a glass plate using a cutting machine. We have developed a DD robot of the SCARA type for shaped glass cutting [2], which includes a computer-aided design (CAD) software package for on-screen designing of the cutting curve. The curve can be made of straight lines, circular arcs, and splines. However, it is usually required by the users to cut a glass plate according to a curve drawn on the paper. To respond to this requirement, we installed a charge-coupled device (CCD) camera on the tip of the DD robot. It guides the robot to move along the curve drawn on the paper and, at the same time, inputs the coordinates data of the curve to the computer. According to these input data, the manipulator can then cut the glass plate into the same shape as the drawing curve. This is shown in Fig. 1. This arrangement makes the manipulator act as a glass-cutting machine, as well as a curve input device.

Manuscript received December 1, 1995; revised October 6, 1998. Abstract published on the Internet March 1, 1999.

The authors are with the Department of Electrical Engineering, Tongji University, Shanghai 200092, China.

Publisher Item Identifier S 0278-0046(99)04150-7.